Expert Systems with Applications 38 (2011) 14148–14155

Contents lists available at ScienceDirect

Expert Systems with Applications

journal homepage: www.elsevier.com/locate/eswa

An adaptive neuro-fuzzy inference system model for predicting the performance of a refrigeration system with a cooling tower

M. Hosoz [a,*], H.M. Ertunc [b], H. Bulgurcu [c]

[a] Department of Mechanical Education, Kocaeli University, 41380 Kocaeli, Turkey
[b] Department of Mechatronics Engineering, Kocaeli University, 41380 Kocaeli, Turkey
[c] Department of Air Conditioning and Refrigeration Technology, Balikesir University, 10023 Balikesir, Turkey

ARTICLE INFO

Keywords:
Refrigeration
Cooling tower
Adaptive neuro-fuzzy inference system (ANFIS)
Prediction

ABSTRACT

This paper investigates the applicability of adaptive neuro-fuzzy inference system (ANFIS) to predict the performance of an R134a vapor-compression refrigeration system using a cooling tower for heat rejection. For this aim, an experimental system was developed and tested at steady state conditions while varying the evaporator load, dry bulb temperature and relative humidity of the air entering the tower, and the flow rates of air and water streams. Then, utilizing some of the experimental data for training, an ANFIS model for the system was developed. This model was used for predicting various performance parameters of the system including the evaporating temperature, compressor power and coefficient of performance. It was found that the predictions usually agreed well with the experimental data with correlation coefficients in the range of 0.807–0.999 and mean relative errors in the range of 0.83–6.24%. The results suggest that the ANFIS approach can be used successfully for predicting the performance of refrigeration systems with cooling towers.

1. Introduction

The vapor-compression refrigeration system with a water-cooled condenser employs a cooling tower to reject the heat absorbed by the water at the condenser to the ambient air. Because the temperature of the water stream leaving the cooling tower is only a few degrees above the ambient wet bulb temperature, this system offers condensing temperatures limited by ambient wet bulb temperature. Consequently, the refrigeration system using a water-cooled condenser operates at lower condenser pressures, thus requiring less compressor power compared with the system using an air-cooled condenser.

Modeling the operation of a refrigeration system requires an elaborate analysis of the heat rejection to the ambient air. Although it is relatively simple to model the heat transfer in an air-cooled condenser, modeling the concurrent heat and mass transfer in a cooling tower is quite difficult. Since the first theoretical analysis of cooling towers performed by Merkel, investigators have developed various mathematical models for estimating the size and thermal performance of forced-flow cooling towers (Bernier, 1994; Braun, Klein, & Mitchell, 1989; Dreyer & Erens, 1996; Fisenko, Brin, & Petruchik, 2004; Halasz, 1999; Soylemez, 1999; Sutherland, 1983; Webb, 1984). However, most of these models utilized experimental data to evaluate transfer coefficients and transfer area. Some of these investigators compared their results with experimental ones, and reported differences usually in the range of 3–15%. On the other hand, the mathematical models of refrigeration systems require a large number of geometrical parameters defining the system, which may not be readily available, and the computer simulations employed in these models are usually complicated due to their dealing with the solution of complex differential equations. Furthermore, the mathematical modeling of cooling towers requires experimental data, and their predictions may not be sufficiently accurate in many cases. Alternatively, the operation of refrigeration systems with cooling towers can be modeled using soft computing techniques such as artificial neural network (ANN) and adaptive neuro-fuzzy inference system (ANFIS) approaches with significantly less engineering effort. These new approaches can extract expertise from data without requiring any explicit mathematical representation, thus easily modeling the physical phenomena in complex systems to predict their behavior under given conditions. Therefore, they can be applied to various engineering problems which are too complex to deal with using classical modeling techniques.

The ANN modeling of air conditioning and refrigeration systems has been studied by many investigators. This approach was used for predicting the performance of the systems or components such as the evaporator (Pacheco-Vega, Sen, Yang, & McClain, 2001), heat pumps (Bechtler, Browne, Bansal, & Kecman, 2001; Esen, Inalli,

* Corresponding author. Tel.: +90 262 3032279; fax: +90 262 3032203.
E-mail address: mhosoz@kocaeli.edu.tr (M. Hosoz).

0957-4174/$ - see front matter © 2011 Elsevier Ltd. All rights reserved.
doi:10.1016/j.eswa.2011.04.225

Nomenclature

A, B	nonlinear parameters in the consequent parts of the fuzzy rules
ANFIS	adaptive neuro-fuzzy inference system
ANN	artificial neural network
A_0	orifice cross section area (m^2)
COP	coefficient of performance
f	output of the fuzzy model
h	specific enthalpy of the refrigerant (kJ kg^{-1})
h_w	specific enthalpy of the water (kJ kg^{-1})
I	current flow through the heaters (A)
K_0	flow coefficient
$\dot{m}$	mass flow rate (kg s^{-1})
MRE	mean relative error
N	number of points in data set or number of independent variables in function R
O	output function
p, q, r	linear parameters in the consequent parts of the fuzzy rules
P_m	orifice differential (mmH_2O)
Q_{cond}	condenser heat rejection rate (W)
Q_e	evaporator load (W)
r	correlation coefficient
R	a function of independent variables
R^2	absolute fraction of variance
RMSE	root mean square error
T	temperature (°C)
V	voltage across the heaters (V)
w	firing strength of a rule
$\overline{w}$	normalized firing strength output
W_{comp}	compressor power (W)
x, y	inputs of the fuzzy model
X	independent variable
Y	expansion factor

Greek symbols

ϕ	relative humidity (%)
μ	membership function
ρ	density (kg m^{-3})
ΔP	orifice pressure drop (Pa)
ω	specific humidity

Subscripts

a	air
$comp$	compressor
$cond$	condenser
dis	compressor discharge
e	evaporator
in	inlet
out	outlet
r	refrigerant
v	water vapor
w	water or wet bulb

Sengur, & Esen, 2008a) liquid chiller (Swider, 2003), ejector-absorption refrigeration system (Sozen, Arcaklioglu, & Ozalp, 2003), vapor-compression refrigeration systems (Arcaklioglu, 2004; Ertunc & Hosoz, 2006; Hosoz & Ertunc, 2006a), automobile air conditioning system (Hosoz & Ertunc, 2006b), and cooling tower (Hosoz, Ertunc, & Bulgurcu, 2007). On the other hand, the application of ANFIS approach to the modeling of thermal systems is a more recent progress although the ANFIS was first introduced in early 90s (Jang, 1993). The ANFIS approach was used for modeling the transient heat transfer in circular duct flow (Hasiloglu, Yilmaz, Comakli, & Ekmekci, 2004), predicting the performance of ground-coupled heat pump systems (Esen, Inalli, Sengur, & Esen, 2007, 2008b), modeling the performance of an evaporative condenser (Ertunc & Hosoz, 2008), predicting the fan speed for energy saving in an HVAC system (Soyguder & Alli, 2009), predicting the heat transfer coefficient in pool boiling of distilled water (Das & Kishor, 2009) and predicting the tip speed ratio in wind turbines (Ata & Kocyigit, 2010).

In this study, the performance of a vapor-compression refrigeration system using R134a as the working fluid and employing a counter-flow cooling tower has been modeled using ANFIS approach. Then, the developed model has been used for predicting various performance parameters of the refrigeration system, including the evaporating temperature, compressor power, coefficient of performance, and the temperature of the water stream leaving the tower.

2. Description and thermodynamic analysis of the experimental setup

The ANFIS approach has been applied to the experimental vapor-compression refrigeration system with a counter-flow cooling tower shown in Fig. 1. The refrigeration system consists of a reciprocating compressor, a shell-and-coil type water-cooled condenser coupled to the cooling tower, a thermostatic expansion valve and an electrically-heated evaporator. The system was charged with 600 g of R134a.

The twin-cylinder open type compressor has a swept volume of 75.7 cm^3 rev^{-1}, and it is belt-driven by a single-phase electric motor. The water-cooled condenser consists of a vertical coil enclosed in welded steel shell, and has a heat transfer area of 0.075 m^2. The evaporator was made from copper tube with two separate electric resistance heaters rolled inside the tube. The refrigeration load is provided to the evaporator by varying the voltage across the electric heaters via a variable transformer.

The cooling tower consists of air and water circuit elements, and a column of packing material through which the two streams are brought into contact with each other. The column is 150 mm × 150 mm × 600 mm high, and it contains eight decks of plastic plates with a total transfer area of 1.14 m^2. A centrifugal fan pulls the ambient air into the tower at a rate determined by the adjustment of the damper setting. After absorbing heat and moisture, the air stream discharges into the atmosphere through an orifice used for measuring airflow rate. A circulation pump draws the cooled water from a tank, and sends it to the water-cooled condenser. The water flow rate can be adjusted by a hand-operated control valve. After absorbing the heat from the condenser, the water stream enters the cooling tower where it is dispensed and let to fall down over the plastic plates. Finally, the cooled water flows into the tank. Because some water evaporates into the air, the water level in the tank is kept constant by adding makeup water to the system through a float-controlled valve.

Fig. 1 also indicates the locations where mechanical and electrical measurements were performed. Mechanical measurements consist of temperature, pressure and mass flow rate measurements, while electrical measurements are the voltage across the electric heaters in the evaporator and current flow through these heaters. Some features of the instrumentation are summarized in Table 1.

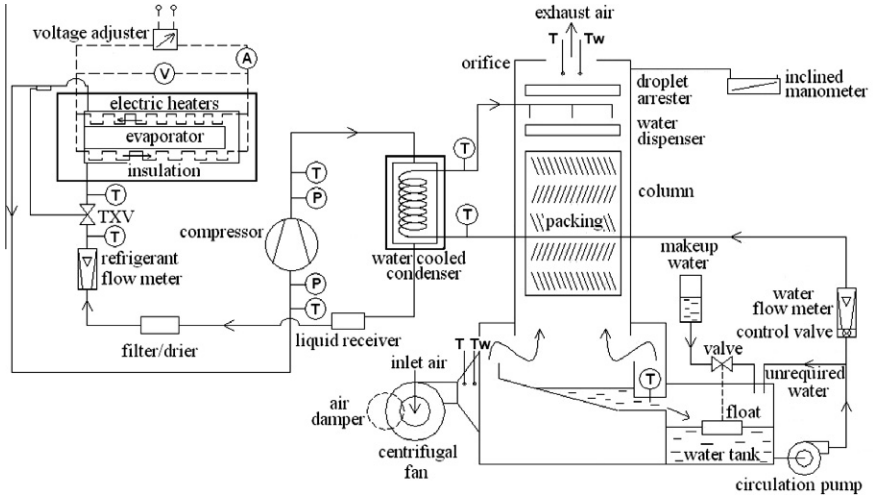

Fig. 1. Schematic diagram of the experimental refrigeration system with a cooling tower.

All temperature measurements were performed using *K*-type thermocouples. The thermocouples for the refrigerant temperature were soldered to the copper tube. Both dry and wet bulb temperatures of the air stream at the inlet and outlet of the cooling tower were measured. The evaporating and condensing pressures were monitored using Bourdon tube gauges. The refrigerant and water mass flow rates were measured with variable-area flow meters. The air mass flow rate through the cooling tower was determined by measuring the pressure difference across the orifice (ΔP) using an inclined manometer, finding the density of the air leaving the tower ($\rho_{a,out}$) with the help of dry and wet bulb temperatures, and evaluating them in the following equation:

$$\dot{m}_a = \rho_{a,out} K_0 A_0 Y \sqrt{\frac{2\Delta P}{\rho_{a,out}}} \tag{1}$$

where K_0 is flow coefficient, A_0 is orifice cross section area and Y is expansion factor. Inserting the values of these three constants into Eq. (1) and defining ΔP as a function of P_m, which stands for the orifice differential in mmH_2O, yields

$$\dot{m}_a \cong 0.0137 \sqrt{P_m \rho_{a,out}} \tag{2}$$

The evaporator load can be evaluated for the refrigerant and the heaters sides:

Table 1
Characteristics of the instrumentation.

Measured variable	Instrument	Range	Accuracy
Refrigerant temperature	Type *K* thermocouple	−50 to100 °C	0.3 °C
Refrigerant pressure	Bourdon gauge	−100 to 600, 0–2000 kPa	5, 20 kPa
Refrigerant flow rate	Variable area flow meter	0–20 g s^{-1}	5%
Air dry bulb temperature	Type *K* thermocouple	0–100 °C	0.3 °C
Air wet bulb temperature	Type *K* thermocouple	0–100 °C	0.3 °C
Air mass flow rate	Orifice-inclined manometer	0–40 mmH_2O	1 mmH_2O
Water mass flow rate	Variable area flow meter	0–50 g s^{-1}	5%
Voltage	Analogue voltmeter	0–250 V	2 V
Current	Analogue ammeter	0–10 A	0.05 A

$$Q_e = \dot{m}_r (h_{e,out} - h_{e,in}) \cong VI \tag{3}$$

As seen in Eq. (3), the evaporator load for the refrigerant side utilizes the refrigerant mass flow rate and refrigerant enthalpies at the outlet and inlet of the evaporator, while that for the heaters side relies on the results of voltage and current measurements. The load deviations between two sides were usually within ±5%, and only the heaters side results were used as the evaporator load due to their having lower uncertainties. Then, the refrigerant mass flow rate based on the evaporator load for the heaters side can be determined from

$$\dot{m}_r = \frac{VI}{h_{e,out} - h_{e,in}} \tag{4}$$

The accuracy for the refrigerant mass flow rate measurements was equal to ±5%, which was poorer than the uncertainty for the flow rates obtained from Eq. (4). Therefore, only the results of this equation were used as the refrigerant flow rate, while the results of direct measurements were used for checking purposes.

Assuming that the compression process is adiabatic, the compressor power absorbed by the refrigerant can be determined from

$$W_{comp} = \dot{m}_r (h_{comp,out} - h_{comp,in}) \tag{5}$$

Assuming that the water-cooled condenser is insulated perfectly, the rate of heat rejected by the refrigerant at the condenser can be equated to the rate of heat absorbed by the water stream:

$$Q_{cond} = \dot{m}_r (h_{cond,in} - h_{cond,out}) \cong \dot{m}_w (h_{w,cond,out} - h_{w,cond,in}) \tag{6}$$

As seen in the above equation, the evaluation of the heat rejection at the condenser for the water side is based on the water mass flow rate and water enthalpies at the outlet and inlet of the condenser. The deviations between two sides were usually within ±5%, and only the refrigerant side results were used as the condenser heat rejection rate.

The ratio of the evaporator load to the compressor power gives the coefficient of performance for the refrigeration system:

$$COP = \frac{Q_e}{W_{comp}} \tag{7}$$

Finally, using the mass flow rate and specific humidities of the air stream entering and leaving the tower, the rate of water evaporated into the air stream in the cooling tower, which is equal to the rate of makeup water, can be evaluated from

$$\dot{m}_v = \dot{m}_a (\omega_{out} - \omega_{in}) \tag{8}$$

In the experimental study, totally 64 different steady state test operations were performed to acquire data for training the proposed ANFIS model and testing its performance. In the tests, the evaporator load was varied between 182 and 455 W, while the dry bulb temperature and relative humidity of the air entering the tower were varied in the ranges of 24.8–39.0 °C and 22.0–52.9%, respectively. On the other hand, the flow rates of the air and water streams passing through the tower were changed between 41.5–90.6 g s^{-1} and 8–30 g s^{-1}, respectively. In order to keep the inlet air temperature and relative humidity at the required values, the refrigeration system along with the cooling tower was located into an air-conditioned laboratory room.

2.1. Uncertainty analysis

The uncertainty analysis for the calculated parameters of the refrigeration system, namely the air and refrigerant mass flow rates, evaporator load, compressor power, condenser heat rejection rate, COP and the rate of water evaporated into the air stream in the cooling tower was performed using the method given by Moffat (1988). According to this method, the function R is assumed to be calculated from a set of totally N measurements (independent variables) represented by

$$R = R(X_1, X_2, X_3, \ldots, X_N) \tag{9}$$

Then the uncertainty of the result R can be determined by combining uncertainties of individual terms using a root-sum-square method, i.e.

$$\delta R = \sqrt{\sum_{i=1}^{N} \left(\frac{\partial R}{\partial X_i} \delta X_i \right)^2} \tag{10}$$

Using the accuracies for various measured variables presented in Table 1, the uncertainties of the calculated parameters were determined with the evaluation of Eqs. (2)–(8) in Eq. (10). The total uncertainties of $\dot{m}_a, \dot{m}_r$ and $\dot{m}_v$ estimated by the analysis are 1.4%, 3.3% and 11.2%, respectively. On the other hand, the total uncertainties of Q_e, W_{comp}, Q_{cond} and COP are estimated as 1.5%, 3.6%, 3.3% and 6.4%, respectively.

3. A brief theoretical background of adaptive neuro-fuzzy inference system

The ANFIS is a multilayer feed-forward network consisting of nodes and directional links, which combines the learning capabilities of a neural network and reasoning capabilities of fuzzy logic. This hybrid structure of the network can extend the prediction capabilities of ANFIS beyond ANN and fuzzy logic techniques when they are used alone. Analyzing the mapping relation between the input and output data, ANFIS can establish the optimal distribution of membership functions using either a backpropagation gradient descent algorithm alone, or in combination with a least squares method.

ANFIS uses the fuzzy if-then rules involving premise and consequent parts of Sugeno type fuzzy inference system (Jang, 1993). In this system, it is simply assumed that the inference system has two inputs x and y and one output f. A typical rule set with two fuzzy *if-then* rules for a first order Sugeno fuzzy model can be expressed as

1. If x is A_1 and y is B_1, then $f_1 = p_1 x + q_1 y + r_1$,
2. If x is A_2 and y is B_2, then $f_2 = p_2 x + q_2 y + r_2$,

where p_1, p_2, q_1, q_2, r_1 and r_2 are linear parameters in the consequent part and A_1, A_2, B_1 and B_2 are nonlinear parameters.

The corresponding equivalent ANFIS architecture for two-input first order Sugeno fuzzy model with two rules is shown in Fig. 2. The architecture of the ANFIS system consists of five layers, namely, the fuzzy layer, product layer, normalized layer, de-fuzzy layer and total output layer. The node functions in the same layer are of the same function family as described in the following (Jang, 1993):

Layer 1: This first layer is called fuzzy layer. The adjustable nodes in this layer are represented by square nodes and marked by A_1, A_2, B_1 and B_2 with x and y outputs. A_1, A_2, B_1 and B_2 are the linguistic labels (small, large, etc.) used in the fuzzy theory for dividing the membership functions. The node function in this layer that determines the membership relation between the input and output functions can be given by

$$O_{1,i} = \mu_{A_i}(x), \quad i = 1, 2 O_{1,j} = \mu_B(y), \quad j = 1, 2 \tag{11}$$

where $O_{1,i}$ and $O_{1,j}$ denote the output functions, and μ_{A_i} and μ_B denote the appropriate membership functions.

Layer 2: This is the product layer and every node is a fixed node marked by a circle node and labeled by Π. The output w_1 and w_2 are the weight functions of the next layer. The output of this layer, $O_{2,i}$, is the product of the input signals and given by

$$O_{2,i} = w_i = \mu_{A_i}(x)\mu_{B_i}(y), \quad i = 1, 2. \tag{12}$$

The output signal of each node, w_i, represents the firing strength of a rule.

Layer 3: This is the normalized layer and every node in this layer is a fixed node, marked by a circle node and labeled by N. The nodes normalize the firing strength by calculating the ratio of firing strength for this node to the sum of all the firing strengths, i.e.

$$O_{3,i} = \overline{w} = \frac{w_i}{w_1 + w_2}, \quad i = 1, 2. \tag{13}$$

Layer 4: This is the de-fuzzy layer having adaptive nodes and marked by square nodes. The node function in this layer is given by a non-fuzzy equation

$$O_{4,i} = \overline{w}_i f_i = \overline{w}_i (p_i x + q_i y + r_i), \quad i = 1, 2. \tag{14}$$

where $\overline{w}_i$ is the normalized firing strength output from the previous layer and $\{p_i, q_i, r_i\}$ is the parameter set of this node. These parameters are linear and referred as consequent parameters of this node.

Layer 5: This is the last layer that simply computes the overall system output as the summation of all incoming signals. Every node in this layer is a fixed node, marked by circle node and labeled by Σ. The node function is given by

$$O_{5,i} = \sum_i \overline{w}_i f_i = \frac{\sum_i \overline{w}_i f}{\sum_i \overline{w}_i}, \quad i = 1, 2. \tag{15}$$

Note that the system output is the weighted sum of the results of the rules. The number of fuzzy sets is determined by the number of nodes in layer 1. On the other hand, the dimension of layer 4 determines the number of fuzzy rules employed in the architecture that shows the complexity and flexibility of the ANFIS architecture.

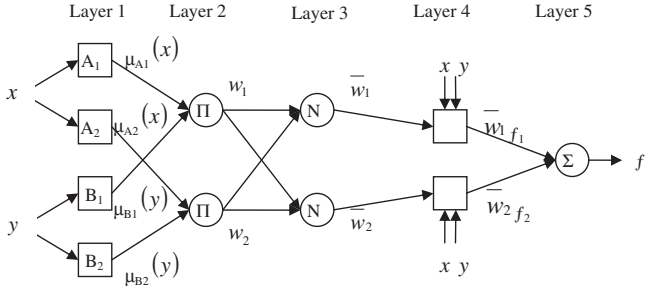

Fig. 2. The architecture of ANFIS.

Similar to ANNs, an ANFIS network can be trained based on supervised learning to reach from a particular input to a specific target output. In the forward pass of the hybrid algorithm of the ANFIS, the node outputs go forward until layer 4 and consequent linear parameters, (p_i, q_i, r_i), are identified by the least-squares method using training data. In the backward pass, the error signals propagate backwards and the premise non-linear parameters, (a_i, b_i, c_i), are updated by gradient descent.

4. Modeling with the ANFIS

In order to develop an ANFIS model for the experimental refrigeration system, the available data set, which consists of 64 input vectors and their corresponding output vectors from the experimental work, was divided into training and test sets. While 75% of the data set was randomly assigned as the training set, the remaining 25% was employed for testing the network performance.

There are five input parameters for the refrigeration system which can influence its outputs: evaporator load (Q_e), dry bulb temperature ($T_{a,in}$) and relative humidity (φ_{in}) of the air stream entering the tower, air mass flow rate ($\dot{m}_a$) and water mass flow rate ($\dot{m}_w$). The output parameters of the refrigeration system with the cooling tower are considered as the refrigerant mass flow rate ($\dot{m}_r$), compressor power (W_{comp}), condenser heat rejection rate (Q_{cond}), coefficient of performance (COP), evaporating temperature (T_e), compressor discharge temperature (T_{dis}), water temperature at the tower outlet ($T_{w,out}$) and mass flow rate of the makeup water ($\dot{m}_v$).

The ANFIS model was developed using MATLAB Fuzzy Logic Toolbox (2002). A subtractive fuzzy clustering was generated to establish a rule base relationship between the input and output parameters. The data was divided into groups called as clusters using the subtractive clustering method to generate fuzzy inference system. In this study, the Sugeno-type fuzzy inference system was implemented to obtain a concise representation of a system's behavior with a minimum number of rules. The linear least square estimation was used to determine each rule's consequent equation. The fuzzy c-means was used as a data clustering technique wherein each data point belongs to a cluster to some degree that is specified by a membership grade. Therefore, a radius value was given in the MATLAB program to specify the cluster center's range of influence to all data dimensions of both input and output. If the cluster radius was specified a small number, then there will be many small clusters in the data that results in many rules. In contrast, specifying a large cluster radius will yield a few large clusters in the data resulting in fewer rules. By trial and error, the cluster radius was determined as 2. Then, the data was trained to identify the parameters of Sugeno-type fuzzy inference system based on the hybrid algorithm combining the least square method and the backpropagation gradient descent method. After training, fuzzy inference calculations of the developed model were performed. Then, the input vectors from the test data set were presented to the trained network and the responses of the network, i.e. the predicted output parameters, were compared with the experimental ones for the performance measurement. The criterions used for measuring the network performance were the correlation coefficient (r), mean relative error (MRE), root mean square error (RMSE) and absolute fraction of variance (R^2). Detailed definitions of these criterions can be found in Ertunc and Hosoz (2006) and Hosoz et al. (2007).

5. Results and discussion

The predictions of the trained ANFIS for the performance parameters of the refrigeration system as a function of the experimental values are shown in Fig. 3. The comparisons in all graphics were made using values only from the test data set, which was not introduced to the ANFIS during the training process. All graphics are provided with a straight line indicating perfect prediction and a ±10 % error band.

As seen in Fig. 3(a), the ANFIS predictions with respect to the experimental values for the refrigerant mass flow rate result in a mean relative error (MRE) of 0.89%, a root mean square error (RMSE) of 0.02 g s^{-1}, a correlation coefficient (r) of 0.999 and an absolute fraction of variance (R^2) of 0.9999 with the experimental data. These results demonstrate that the ANFIS predicts the refrigerant mass flow rate quite well despite wide ranges of operating conditions.

Because the evaluation of the compressor power requires the refrigerant mass flow rate and refrigerant enthalpies at the inlet and outlet of the compressor, it involves several sources of uncertainty. Consequently, the resultant high uncertainty influences the training process, thus, as reported in Fig. 3(b), yielding a relatively poorer performance for the W_{comp} predictions compared with $\dot{m}_r$ ones.

It is seen in Fig. 3(c) that the ANFIS predicts the condenser heat rejection rate very well. However, the performance of ANFIS for the COP predictions is slightly poor, as revealed in Fig. 3(d). This is due to the fact that the COP depends on two parameters, namely the evaporator load and compressor power. Because of various uncertainty sources involved in the evaluation of these parameters, the COP has a high uncertainty, as depicted in Section 2.1. This leads to relatively poor training, which in turn causes a poor statistical performance for the COP predictions.

Fig. 3(e) shows that the ANFIS predictions for the evaporating temperature have a very low RMSE and a high correlation coefficient along with a moderate MRE of 2.80%. Because the temperature of the refrigerated medium is related to the evaporating temperature, the ANFIS predicting T_e accurately would also be successful in predicting the temperature of the refrigerated medium in a more realistic application.

Fig. 3(f) indicates that the ANFIS predictions for the compressor discharge temperature yield a lower MRE although it gives a higher RMSE and a lower correlation coefficient compared with T_e predictions. The discharge temperature is an indicator of the compressor durability. The possibility of the thermal destruction of the compressor oil increases with rising discharge temperature.

The ANFIS predictions for the temperature of the water stream leaving the cooling tower and the mass flow rate of water evaporated into the air stream in the tower as a function of the experimental values are shown in Fig. 4(a) and (b), respectively. The ANFIS yields outstanding predictions for $T_{w,out}$ with a MRE of 0.83%, a RMSE of 0.26 °C, a correlation coefficient of 0.990 and an absolute fraction of variance of 0.9999. On the other hand, the ANFIS predictions for $\dot{m}_v$ are slightly poorer. This can be attributed to the fact that $\dot{m}_v$ was evaluated from the measurements of air mass flow rate along with dry and wet bulb temperatures at the tower inlet and outlet. Consequently, the ANFIS trained with $\dot{m}_v$ data of high uncertainty results in a poor prediction performance.

The comparisons of the ANFIS predictions for the eight output parameters with the experimental results are alternatively presented in Fig. 5. It is seen that the test patterns consist of the results of 16 tests and the ANFIS remarkably predicts all of the output parameters in almost the entire range of the experiments. It is obvious that if a higher number of test runs had been performed to provide a larger amount of experimental data for training, the ANFIS would have performed even better.

The versatility of ANFIS modeling can be noticed easily when the ANFIS is used for investigating the effects of the input parameters on the outputs. For this aim, the predictions of the ANFIS model for the COP and T_e as a function of the evaporator load and mass flow rate of the water stream circulating through the

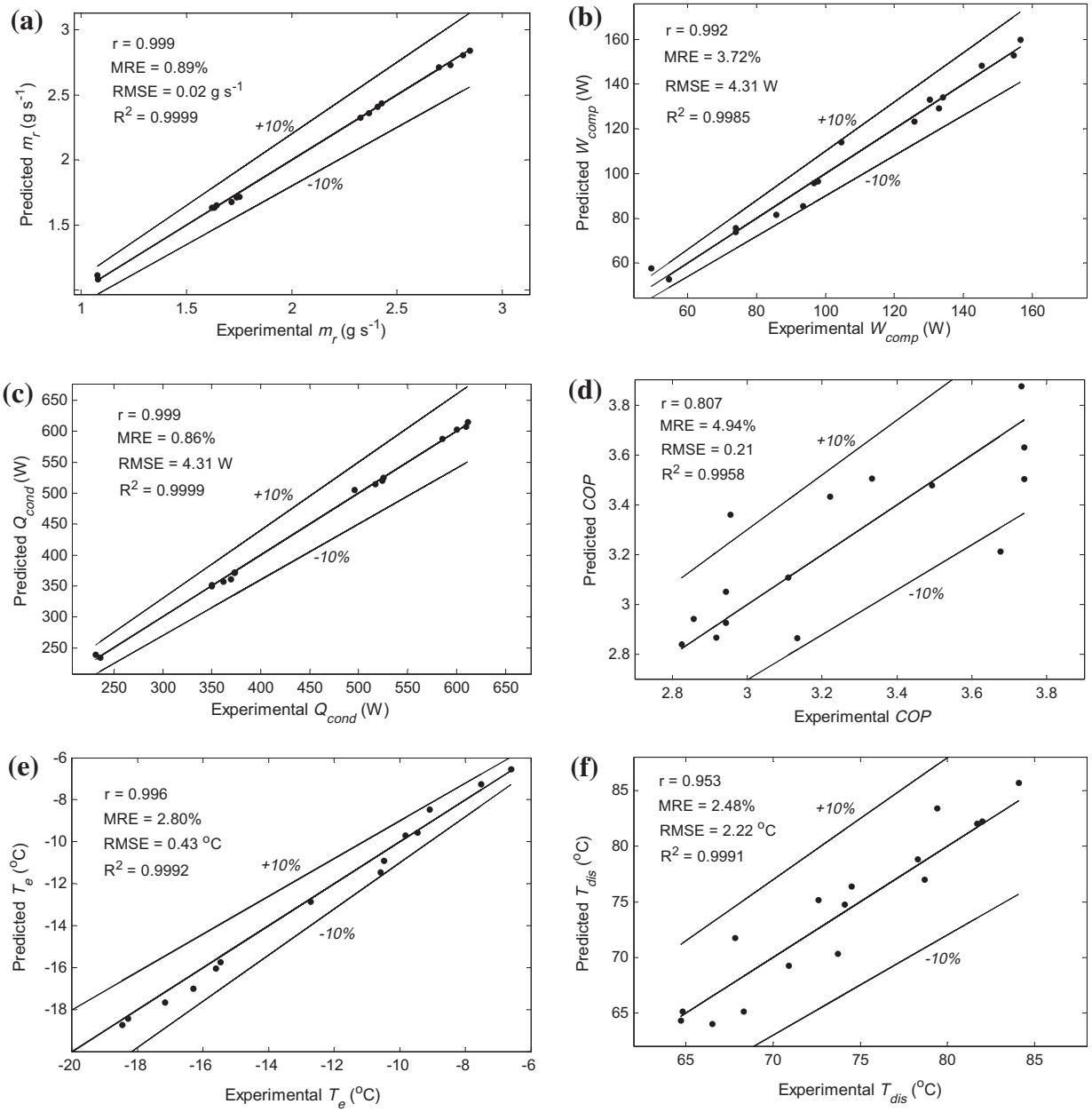

Fig. 3. The ANFIS predictions for the performance parameters of the refrigeration circuit vs. experimental values.

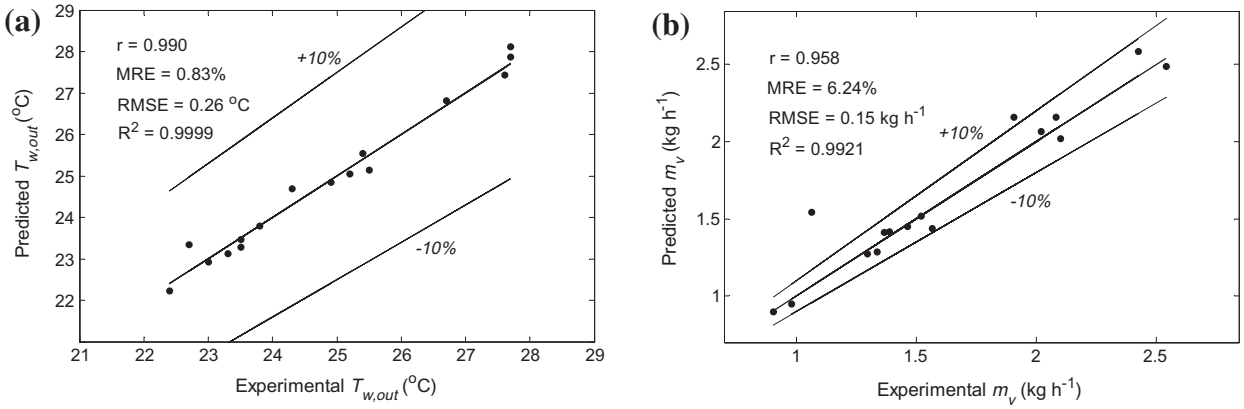

Fig. 4. The ANFIS predictions for the performance parameters of the cooling tower vs. experimental values.

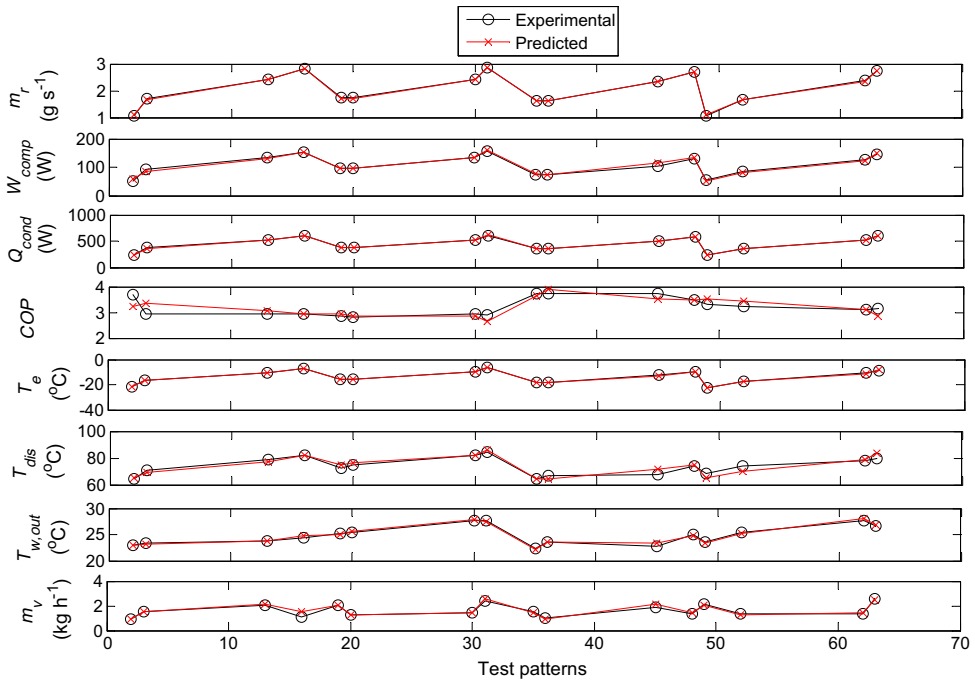

Fig. 5. Comparisons of the ANFIS predictions and experimental results for various test patterns.

system are presented in Figs. 6 and 7, respectively, as sample results. Note that Figs. 6 and 7 report the predictions not only in the considered input range of the experimental study but also those beyond the range of the experiments.

Fig. 6 indicates the changes in the predicted values of *COP* and T_e with respect to the evaporator load when other four input parameters are kept constant at the values shown in the figure. As expectedly, *COP* and T_e rise with increasing Q_e. Because the points in Fig. 6 were not obtained experimentally, the accuracies of these predictions can not be measured. However, the statistical prediction performance of the developed ANFIS model has already been presented in Figs. 3 and 4.

Fig. 7 shows the changes in the predicted values of *COP* and T_e with respect to the water mass flow rate circulating through the system when other four input parameters are kept constant at the values shown in the figure. It is observed that T_e drops slightly while COP rises moderately with increasing $\dot{m}_w$. The higher the $\dot{m}_w$, the higher the rate of water evaporated into the air stream. This higher amount of evaporated water absorbs more heat from the remaining water mass, thus cooling it to a lower temperature. Then, the condensing temperature and pressure decreases with lowering water temperature. Accompanying the drop in the condensing temperature, the evaporating temperature decreases with increasing $\dot{m}_w$. Furthermore, the lowered condensing pressure causes a drop in the compressor power, thus yielding a rising *COP*.

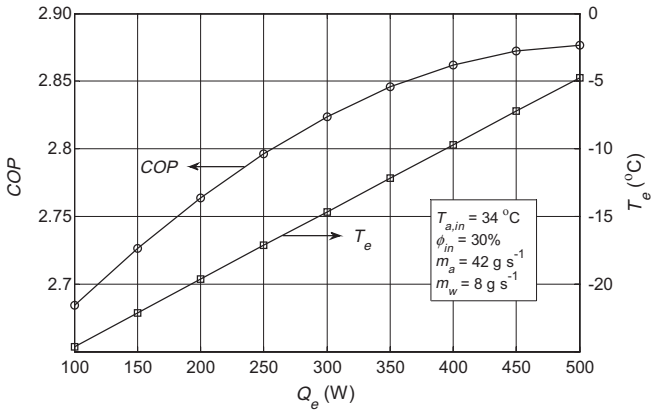

Fig. 6. The ANFIS predictions for the coefficient of performance and evaporating temperature vs. evaporator load.

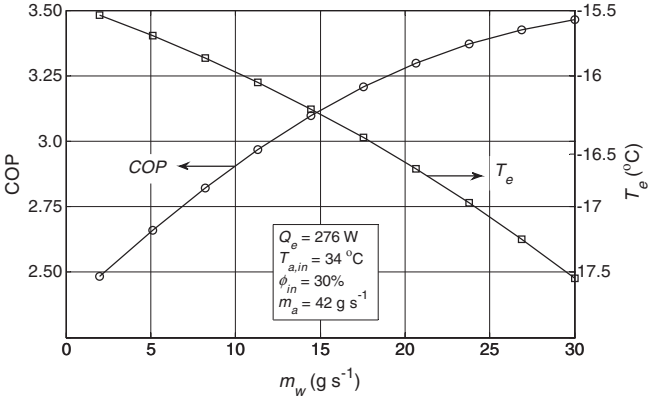

Fig. 7. The ANFIS predictions for the coefficient of performance and evaporating temperature vs. flow rate of the water stream passing through the tower.

6. Conclusions

The use of ANFIS modeling technique for predicting the performance of a refrigeration system with a cooling tower has been studied. For this aim, an experimental refrigeration system was tested under different operating conditions to obtain 64 input–output pairs. Then, an ANFIS model for the system was developed to predict its various performance parameters. The performance of the ANFIS predictions was measured using the correlation coefficient, mean relative error, root mean square error and absolute fraction of variance. The ANFIS model usually yielded a good statistical performance with the correlation coefficients in the range of

0.807–0.999, MREs in the range of 0.83–6.24% and absolute fractions of variance in the range of 0.9921–0.9999. Finally, using the developed model, the effects of the evaporator load and mass flow rate of the water stream circulating through the system on some of the output parameters were investigated.

The results reveal that refrigeration systems with cooling towers can be modeled accurately using the ANFIS approach. This new technique requires only a limited number of tests instead of a comprehensive experimental study or dealing with a complex mathematical model. Consequently, engineers relying on the ANFIS technique for determining the performance of refrigeration systems can save both time and funds.

References

Arcaklioglu, E. (2004). Performance comparison of CFCs with their substitutes using artificial neural network. *International Journal of Energy Research, 28*, 1113–1125.

Ata, R., & Kocyigit, Y. (in press). An adaptive neuro-fuzzy inference system approach for prediction of tip speed ratio in wind turbines. *Expert Systems with Applications*. doi:10.1016/j.eswa.2010.02.068.

Bechtler, H., Browne, M. W., Bansal, P. K., & Kecman, V. (2001). Neural networks – A new approach to model vapour-compression heat pumps. *International Journal of Energy Research, 25*, 591–599.

Bernier, M. A. (1994). Cooling tower performance: Theory and experiments. *ASHRAE Transactions, 100*, 114–121.

Braun, J. E., Klein, S. A., & Mitchell, J. W. (1989). Effectiveness models for cooling towers and cooling coils. *ASHRAE Transactions, 95*, 164–174.

Das, M. K., & Kishor, N. (2009). Adaptive fuzzy model identification to predict the heat transfer coefficient in pool boiling of distilled water. *Expert Systems with Applications, 36*, 1142–1154.

Dreyer, A. A., & Erens, P. J. (1996). Modelling of cooling tower splash pack. *International Journal of Heat Mass Transfer, 39*, 109–123.

Ertunc, H. M., & Hosoz, M. (2006). Artificial neural network analysis of a refrigeration system with an evaporative condenser. *Applied Thermal Engineering, 26*, 627–635.

Ertunc, H. M., & Hosoz, M. (2008). Comparative analysis of an evaporative condenser using artificial neural network and adaptive neuro-fuzzy inference system. *International Journal of Refrigeration, 31*, 1426–1436.

Esen, H., Inalli, M., Sengur, A., & Esen, M. (2007). Modelling a ground-coupled heat pump system using adaptive neuro-fuzzy inference system. *International Journal of Refrigeration, 31*, 65–74.

Esen, H., Inalli, M., Sengur, A., & Esen, M. (2008a). Forecasting of a ground-coupled heat pump performance using neural networks with statistical data weighting pre-processing. *International Journal of Thermal Sciences, 47*, 431–441.

Esen, H., Inalli, M., Sengur, A., & Esen, M. (2008b). Artificial neural networks and adaptive neuro-fuzzy assessments for ground-coupled heat pump system. *Energy and Buildings, 40*, 1074–1083.

Fisenko, S. P., Brin, A. A., & Petruchik, A. I. (2004). Evaporative cooling of water in mechanical draft cooling tower. *International Journal of Heat and Mass Transfer, 47*, 165–177.

Halasz, B. (1999). Application of a general non-dimensional mathematical model to cooling towers. *International Journal of Thermal Sciences, 38*, 75–88.

Hasiloglu, A., Yilmaz, M., Comakli, O., & Ekmekci, I. (2004). Adaptive neuro-fuzzy modeling of transient heat transfer in circular duct air flow. *International Journal of Thermal Sciences, 43*, 1075–1090.

Hosoz, M., & Ertunc, H. M. (2006a). Modelling of a cascade refrigeration system using artificial neural network. *International Journal of Energy Research, 30*, 1200–1215.

Hosoz, M., & Ertunc, H. M. (2006b). Artificial neural network analysis of an automobile air conditioning system. *Energy Conversion and Management, 47*, 1574–1587.

Hosoz, M., Ertunc, H. M., & Bulgurcu, H. (2007). Performance prediction of a cooling tower using artificial neural network. *Energy Conversion Management, 48*, 1349–1359.

Jang, J. (1993). ANFIS: Adaptive network-based fuzzy inference systems. *IEEE Transactions on Systems, Man and Cybernetics, 23*, 665–685.

MATLAB Documentation (2002). *Fuzzy toolbox user's guide of MATLAB*. The MathWorks, Inc.

Moffat, R. J. (1988). Describing the uncertainties in experimental results. *Experimental Thermal and Fluid Science, 1*, 3–17.

Pacheco-Vega, A., Sen, M., Yang, K. T., & McClain, R. L. (2001). Neural network analysis of fin-tube refrigerating heat exchanger with limited experimental data. *International Journal of Heat and Mass Transfer, 44*, 763–770.

Soyguder, S., & Alli, A. (2009). Predicting of fan speed for energy saving in HVAC system based on adaptive network based fuzzy inference system. *Expert Systems with Applications, 36*, 8631–8638.

Soylemez, M. S. (1999). Theoretical and experimental analyses of cooling towers. *ASHRAE Transactions, 105*, 330–337.

Sozen, A., Arcaklioglu, E., & Ozalp, M. (2003). A new approach to thermodynamic analysis of ejector-absorbtion cycle: Artificial neural networks. *Applied Thermal Engineering, 23*, 937–952.

Sutherland, J. W. (1983). Analysis of mechanical draught counterflow air/water cooling towers. *Journal of Heat Transfer, 105*, 576–583.

Swider, D. J. (2003). A comparison of empirically based steady-state models for vapour-compression liquid chillers. *Applied Thermal Engineering, 23*, 539–556.

Webb, R. L. (1984). A unified theoretical treatment for thermal analysis of cooling towers, evaporative condensers, and fluid coolers. *ASHRAE Transactions, 90*, 398–415.